

Electron scattering form factors from exotic nuclei

S. Karataglidis^{(a)*} and K. Amos^{(b)†}

^(a) Department of Physics and Electronics, P.O. Box 94,
Rhodes University, Grahamstown, 6140, South Africa and

^(b) School of Physics, University of Melbourne, Victoria, 3010, Australia.

(Dated: October 29, 2018)

Abstract

The elastic electron scattering form factors, longitudinal and transverse, from the He and Li isotopes and from ${}^8\text{B}$ have been studied. Large space shell model functions have been assumed. The precise distribution of the neutron excess has little effect on the form factors of the isotopes though there is a mass dependence in the charge densities. However, the form factors of the proton-rich nucleus, ${}^8\text{B}$, are significantly changed by the presence of the proton halo.

PACS numbers: 21.10.Ft,21.60.Cs,25.30.Bf

The form factors from elastic electron scattering off exotic nuclei is of topical interest given the proposed construction of an electron-ion collider at GSI [1] and the effort to measure electron scattering form factors of exotic nuclei at RIKEN using Self-Confining Radioactive Ion Targets (SCRITs) [2]. Such experiments will provide direct information of the charge distributions in exotic nuclei that lie outside of the valley of stability and whose structures may have skins or halos for the excess nucleons. Also, through appropriate kinematic selection of collision events, those facilities may obtain transverse as well as longitudinal form factors. Taken together with analyses of nucleon-nucleus (NA) scattering data which provide information on the matter densities [3], analyses of these form factors should make feasible a significant map of the densities of exotic nuclei.

Electron scattering from exotic nuclei has been considered previously by Antonov *et al.* [4], for both light and heavy systems. In particular, for scattering from light nuclei, they used a Helm model to obtain longitudinal form factors. Therein densities obtained from no-core shell model calculations [5, 6] also were used. With the He isotopes, they found that the charge density of ${}^6\text{He}$ differed from that of ${}^4\text{He}$ but that of ${}^8\text{He}$ was not significantly different to that of ${}^6\text{He}$. They also noted that the proton density does extend far with increasing neutron number. However, they did not make any conclusion as to the role of the neutron halo character of ${}^6\text{He}$. That role, of the halo in elastic electron scattering, was sought more recently by Bertulani [7]. He also used the Helm model and found that the contribution from the neutron halo itself was insignificant. However, for proton-rich nuclei, he observed that the proton halo did so, and significantly. That is to be expected given the large extension of the charge density over that of a skin such a halo engenders.

As those recent works [4, 7] used the Helm model, only the longitudinal form factors could be considered. Essentially they are the Fourier transforms of the charge density. It is the purpose of this letter to consider both the longitudinal and transverse elastic electron scattering form factors for the He and Li isotopes from the valley of stability to the drip lines and to use a large space no-core shell model to define the required structure information. For comparison, we have studied the form factors of the proton-halo nucleus, ${}^8\text{B}$.

The microscopic model for electron scattering specified by deForest and Walecka [8] and by Karatagliidis, Halse and Amos [9] and based on the shell model, has been used to calculate the form factors. Using the notation of the latter, the form factors for electron scattering between nuclear states J_i and J_f involving angular momentum transfer J are expressed as

$$|F_J^\eta(q)|^2 = \frac{1}{2J_i + 1} \left(\frac{4\pi}{Z^2} \right) |\langle J_f \parallel T_J^\eta(q) \parallel J_i \rangle|^2, \quad (1)$$

where η selects the type, i.e. longitudinal, transverse electric, or transverse magnetic. Assuming one-body operators, the reduced matrix elements may be expressed in the form,

$$\langle J_f \parallel T_J^\eta(q) \parallel J_i \rangle = \frac{1}{\sqrt{2J + 1}} \text{Tr}(SM), \quad (2)$$

where S is the matrix of one-body transition densities, $S_{j_1 j_2 J}$, defined as

$$S_{j_1 j_2 J} = \left\langle J_f \left\| \left[a_{j_2}^\dagger \times \tilde{a}_{j_1} \right]^J \right\| J_i \right\rangle. \quad (3)$$

M denotes the matrix elements of the one-body longitudinal or transverse electromagnetic operators for each allowed particle-hole excitation ($j_2-j_1^{-1}$). Bare operators are used for the

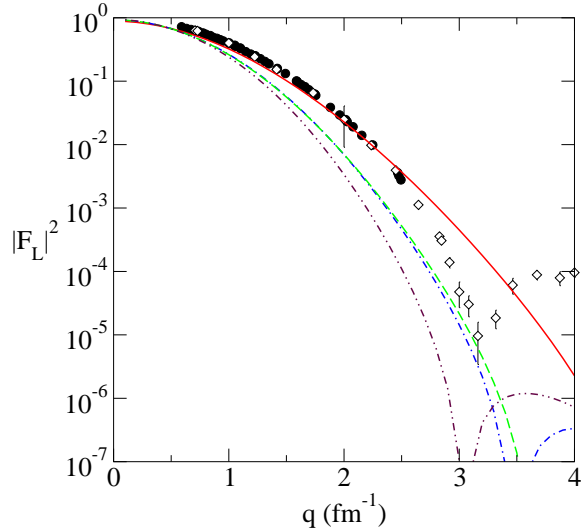


FIG. 1: (Color online.) Elastic electron scattering form factors for ^4He (solid line), ^6He (dashed line, halo; dot-dashed line, non-halo), and ^8He (double dot-dashed line). The data for the ^4He form factor are those of McCarthy *et al.* [14].

results presented herein, and explicit meson-exchange-current (MEC) effects are ignored. However, MEC have been incorporated implicitly in the transverse electric form factors in the long-wave limit by using Siegert's theorem [10]. That serves to introduce into the transverse electric form factor an explicit dependence on the charge density, through the use of the continuity equation. Hence, any effect on the charge density from a halo would affect both longitudinal and transverse electric form factors.

Within the framework of the shell model, the halo has been specified by using Woods-Saxon (WS) single-particle (SP) wave functions with the binding energies of the orbits occupied by the valence (halo) nucleons set to the appropriate single-nucleon separation energies. Doing so allows for the extension of the nucleon density consistent with there being a halo [6]. Conversely, when the density is specified using harmonic oscillator (HO) wave functions, consistent with the shell model, a neutron skin results. Hence, results obtained with WS and HO SP wave functions are denoted as halo and non-halo, respectively. This distinction is not new. It has been used to explain the anomalously large $B(E1)$ value for ^{11}Be with simple shell model wave functions [11]. Also, such a distinction has allowed identification of the halo attribute in ^6He in analyses of elastic and inelastic scattering of ^6He from hydrogen [12].

We first discuss the form factors for electron scattering from the even-even He isotopes. The shell model wave functions for $^{4,6,8}\text{He}$ were obtained from a complete $(0+2+4)\hbar\omega$ shell model using the G matrix shell model interactions of Zheng *et al.* [13]. The halo in ^6He was specified by using WS wave functions with the SP energies of the $0p$ -shell neutrons set to the single neutron separation energy of 1.8 MeV [6]. An oscillator parameter of 1.8 fm was used to specify the HO SP wave functions.

The longitudinal elastic electron scattering form factors from the He isotopes are displayed in Fig. 1. Therein, the form factors for the scattering from ^4He and ^8He are portrayed by the solid and double-dot-dashed lines, while the results of the calculations made using the halo and non-halo models of ^6He are given by the dashed and dot-dashed lines respectively. The data for the ^4He form factor are those of McCarthy *et al.* [14]. The comparison of the

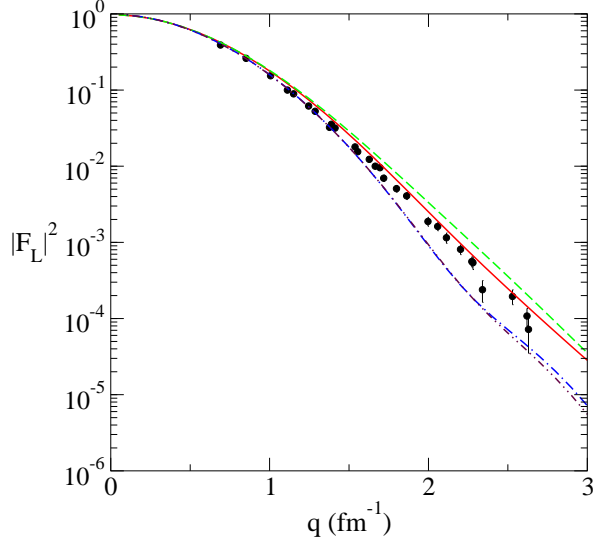


FIG. 2: (Color online.) The longitudinal elastic scattering form factors for ^7Li , ^9Li , and ^{11}Li . The results of the calculations made for ^7Li , ^9Li , and ^{11}Li are portrayed by the solid, dashed, and dot-dashed (non-halo) and double-dot-dashed (halo) lines. The data for the ^7Li longitudinal form factor are from Refs. [16, 17].

^4He form factor with data is quite good up to 2.5 fm^{-1} . This is consistent with the predicted charge radius of 1.71 fm as compared to the measured value of $1.671 \pm 0.014 \text{ fm}$ [15]. The addition of neutrons to form ^6He and ^8He pull the charge density out and thus the form factors decrease with momentum transfer. Note that there is little difference between the results of the halo and non-halo calculations for the ^6He form factor. The form factor is not dependent on detailed properties of the neutron halo. It is only the presence of the extra 2 neutrons that causes the change to the proton distribution. The Helm model results of Antonov *et al.* [4] for the ^6He form factor generally agree with the present ones. However, Antonov *et al.* [4] under-predict the ^4He form factor as compared to the transform of the experimental charge density, and somewhat over-predict the ^8He form factor. It would seem that, while the charge densities of the isotopes are essentially the same, that they have used for ^4He is too extended.

The longitudinal elastic scattering form factors for ^7Li , ^9Li , and ^{11}Li are displayed in Fig. 2. The level of agreement between the results of our calculations for ^7Li with the data of Suelzle *et al.* [16] and of Lichtenstadt *et al.* [17] is quite good. The addition of two neutrons to ^7Li does not change the form factor substantially and so the charge density for ^9Li is little changed from that for ^7Li . But a noticeable change is observed in the form factor for ^{11}Li . It decreases faster than the other two with increasing momentum transfer. As with ^6He , this extension of the charge density does not come about with the halo specifics in this nucleus. Rather, it is due only to the coupling of the 4 extra neutrons to the ^7Li core. A similar conclusion has been reached by Bertulani [7].

The transverse elastic scattering form factors for ^7Li , ^9Li , and ^{11}Li are displayed in Fig. 3. These form factors are dominated by $M1$ effects at low momentum transfer values, to $\sim 1 \text{ fm}^{-1}$, but are dominated by $E2$ contributions above that value [5]. The $M1$ form factors for all three nuclei are quite similar. It is dominated entirely by the proton contribution. Such is expected as that form factor is not influenced by changes in the charge density. The

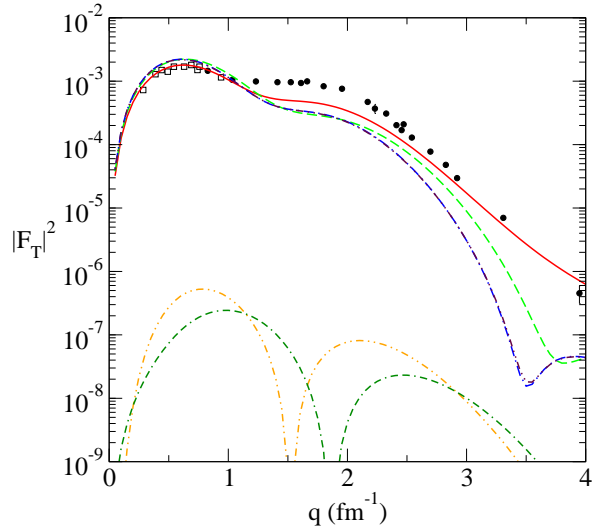


FIG. 3: (Color online.) As for Fig. 2 but for the transverse form factors. The data are from Refs. [17, 18]. The halo and nonhalo neutron components of the M1 form factor from ^{11}Li are portrayed by the double-dot-dashed and dot-double-dashed lines, respectively, at the bottom of the figure.

neutron contribution to the ^{11}Li $M1$ form factor, also shown in Fig. 3, is influenced by the neutron halo but is several orders of magnitude below the proton component. The $E2$ form factor shows significant decreases in value at large momentum transfers for both ^9Li and ^{11}Li from the reference ^7Li form factor. As with the longitudinal ^{11}Li form factor, that decrease is due only to the addition of the 4 neutrons about the ^7Li core and not due to the halo characteristic.

As a comparison to the neutron halos, we now consider electron scattering from a proton halo nucleus, namely ^8B . A complete $(0 + 2 + 4)\hbar\omega$ shell model using the Zheng interaction [13] was used to obtain the OBDME. The single proton separation energy from ^8B is 137 keV [19] and the halo is specified by using WS functions for $0p$ -shell protons with that binding energy. The non-halo specification uses the same set of WS functions as for ^8He . The prediction for the longitudinal elastic electron scattering form factor from ^8B is presented in Fig. 4. This form factor is dominated by the $C0$ component below 1 fm^{-1} while the $C2$ contribution becomes significant above that value. The $C4$ component is negligible. The effect of the proton halo, in this case, is very evident with the decrease in the form factor with momentum transfer reflecting the more extensive charge distribution.

The transverse elastic scattering form factor for ^8B is shown in Fig. 5. The effect of the proton halo on this form factor for ^8B is just as dramatic as that on the longitudinal one. The change in this case is a significant decrease in all components of the form factor. As it is dominated by the $E2$ component, the total transverse form factor decreases markedly due to the presence of the halo. The magnetic components are also significantly modified by the proton halo, although that manifests itself only in a change at very low momentum transfer where the $M1$ component dominates.

Results have been presented for the elastic electron scattering form factors from exotic nuclei to elicit details of the effects of the extended nucleon matter distributions on the charge density. Significantly, the neutron halo character does not influence the electron scattering form factors, as was shown in reference to the form factors of ^6He and ^{11}Li . Instead, the

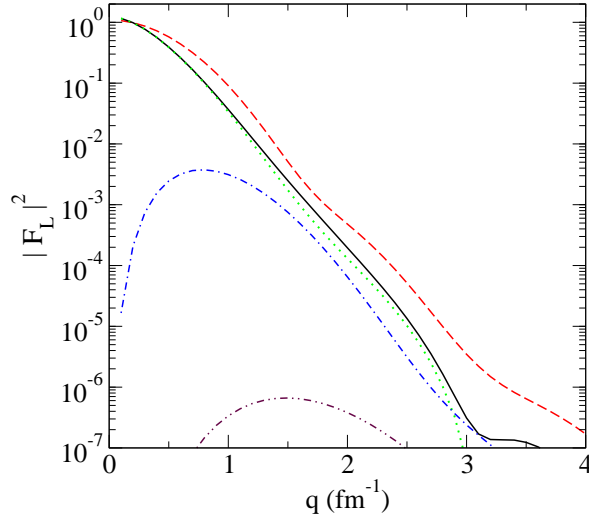


FIG. 4: (Color online.) Longitudinal elastic scattering form factor for ${}^8\text{B}$. The halo and non-halo model results are portrayed by the solid and dashed lines, respectively. The $C0$, $C2$, and $C4$ components of the halo form factor are given by the dotted, dot-dashed, and double-dot-dashed lines, respectively.

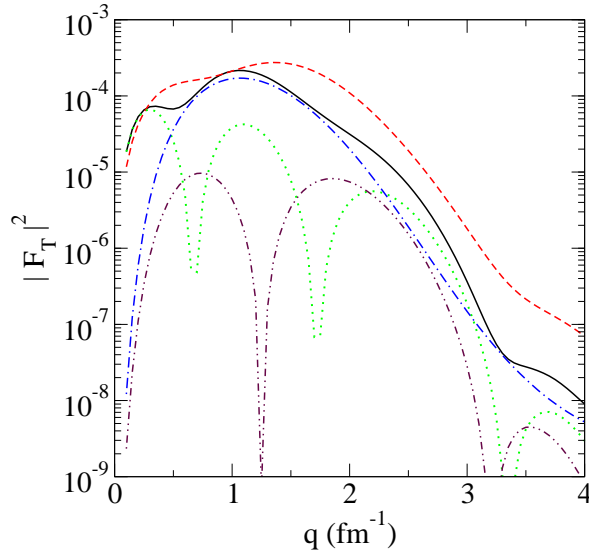


FIG. 5: (Color online.) Transverse elastic scattering form factor for ${}^8\text{B}$. The form factors from the halo and non-halo calculations are given by the solid and dashed lines. The $M1$, $E2$, and $M3$ form factors are given by the dotted, dot-dashed, and double-dot-dashed lines, respectively.

charge density is extended naturally only through the addition of neutrons to the stable isotopes. That will occur irrespective of whether the exotic nucleus has a neutron halo or a neutron skin.

The situation for proton halos is entirely different. The longitudinal and transverse electron scattering form factors for ${}^8\text{B}$ are significantly reduced compared to the standard shell model result. This is consistent with the extension of the charge density due to the proton halo. The transverse form factors portrays similar behavior due to the dominance of

the $E2$ component, which is also affected by the proton halo.

With the prospect of electron scattering form factors being measured soon with SCRIT [2] or the electron-ion collider [1], it is hoped that investigations of the proton halos will be possible. Transverse form factors should also be measured as such measurements will also be possible in the collider. Analysis with complementary RIB-hydrogen scattering data then suggests the possibility of a significant mapping of the densities of exotic nuclei so providing detailed microscopic tests of structure models in use.

* Electronic address: S.Karataglidis@ru.ac.za

† Electronic address: amos@physics.unimelb.edu.au

- [1] *Technical Proposal for the Design, Construction, Commissioning, and Operation of the ELISE setup*, spokesperson Haik Simon, GSI Internal Report, Dec. 2005.
- [2] T. Suda and M. Wakasugi, *Prog. Part. Nucl. Phys.* **55**, 417 (2005).
- [3] K. Amos, P. J. Dortmans, H. V. von Geramb, S. Karataglidis, and J. Raynal, *Adv. in Nucl. Phys.* **25**, 275 (2000).
- [4] A. N. Antonov, D. N. Kadrev, M. K. Gaidarov, E. Moya de Guerra, P. Sarriguren, J. M. Udiás, V. K. Lukyanov, E. Zemlyanaya, and G. Z. Krumova, *Phys. Rev. C* **72**, 044307 (2005).
- [5] S. Karataglidis, P. G. Hansen, B. A. Brown, K. Amos, and P. J. Dortmans, *Phys. Rev. Lett.* **79**, 1447 (1997).
- [6] S. Karataglidis, P. J. Dortmans, K. Amos, and C. Bennhold, *Phys. Rev. C* **61**, 024319 (2000).
- [7] C. A. Bertulani (2006), nucl-th/0604044.
- [8] T. deForest and J. D. Walecka, *Adv. Phys.* **15**, 1 (1966).
- [9] S. Karataglidis, P. Hulse, and K. Amos, *Phys. Rev. C* **51**, 2494 (1995).
- [10] J. L. Friar and W. C. Haxton, *Phys. Rev. C* **31**, 2027 (1985).
- [11] D. J. Millener, J. W. Olness, E. K. Warburton, and S. S. Hanna, *Phys. Rev. C* **28**, 497 (1983).
- [12] A. Lagoyannis et al., *Phys. Lett.* **B518**, 27 (2001).
- [13] D. C. Zheng, B. R. Barrett, J. P. Vary, W. C. Haxton, and C.-L. Song, *Phys. Rev. C* **52**, 2488 (1995).
- [14] J. S. McCarthy, I. Sick, and R. R. Whitney, *Phys. Rev. C* **15**, 1396 (1977).
- [15] C. R. Ottermann, G. Köbschall, K. Maurer, K. Rörich, C. Schmitt, and V. H. Walter, *Nucl. Phys.* **A436**, 688 (1985).
- [16] L. R. Suelzle, M. R. Yearian, and H. Crannell, *Phys. Rev.* **162**, 992 (1967).
- [17] J. Lichtenstadt, J. Alster, M. A. Moinester, J. Dubach, R. S. Hicks, G. A. Peterson, and S. Kowlaski, *Phys. Lett.* **B219**, 394 (1989).
- [18] G. J. C. van Niftrik, L. Lapikás, H. de Vries, and G. Box, *Nucl. Phys.* **A174**, 173 (1971).
- [19] D. R. Tilley, J. H. Kelley, J. L. Godwin, D. J. Millener, J. E. Purcell, C. G. Sheu, and H. R. Weller, *Nucl. Phys.* **A745**, 155 (2004).